Physics Procedia

Volume 75, 2015, Pages 221–229

20th International Conference on Magnetism

Muon-Spin Rotation in Multiferroic $Cu_3Mo_2O_9$ under Electric Fields

Haruhiko Kuroe[1,2], Hideki Kuwahara[1], Tomoyuki Sekine[1], Isao Watanabe[2], Andrea-Raeto Raselli[3], Matthias Elender[3], Pabitra Kumar Biswas[3], Masashi Hase[4], Kunihiko Oka[5], Toshimitsu Ito[5], and Hiroshi Eisaki[5]

[1] Sophia University, Tokyo 102-8554, Japan
[2] RIKEN Nishina Center, Wako, Saitama 351-0198, Japan
[3] Paul Scherrer Institute (PSI), 5232 Villigen PSI, Switzerland
[4] National Institute for Materials Science (NIMS), Tsukuba 305-0047, Japan
[5] National Institute of Advanced Industrial Science and Technology (AIST), Tsukuba 305-8562, Japan

Abstract

It has been demonstrated that the muon spin rotation measurements under electric field give helpful information about the electrically induced magnetism, e.g., the cross correlation effects in multiferroic materials. We have developed an electric-field application system up to 500 V for the Dolly spectrometer at the Paul Scherrer Institute. We report the electric-field effects on the μSR spectrum in the multiferroic material $Cu_3Mo_2O_9$, where a slightly canted antiferromagnetic long-range order appears together with the ferroelectricity below 8 K. In the muon-spin rotation spectrum at 1.5 K, two kinds of the internal magnetic fields are clearly observed as a beating oscillation. The muon-spin spectrum depends on the electric fields along the c axis of the crystal along which the spontaneous electric polarization appears. From the fitting of the spectra in time and frequency domains, it is shown that the observation of the electric-field dependence on the muon-spin spectra clearly indicates a change of the internal magnetic fields induced by the application of the external electric fields. We propose a model with one muon-stopping site which explains the observed spectra qualitatively. This model is based on the magnetic excitations in $Cu_3Mo_2O_9$ obtained from the inelastic neutron-scattering experiments.

Keywords: multiferroic materials, muon spin rotation (μSR), cross correlation

1 Introduction

Multiferroic materials and their cross correlation effects have been extensively studied after the historical paper which reported the magnetic control of ferroelectric polarization [1]. Because the cross correlation effects contain the seeds of future applications, these are widely studied not only in viewpoints of science but also of device developments.

Selection and peer-review under responsibility of the Scientific Programme Committee of ICM 2015

doi:10.1016/j.phpro.2015.12.195

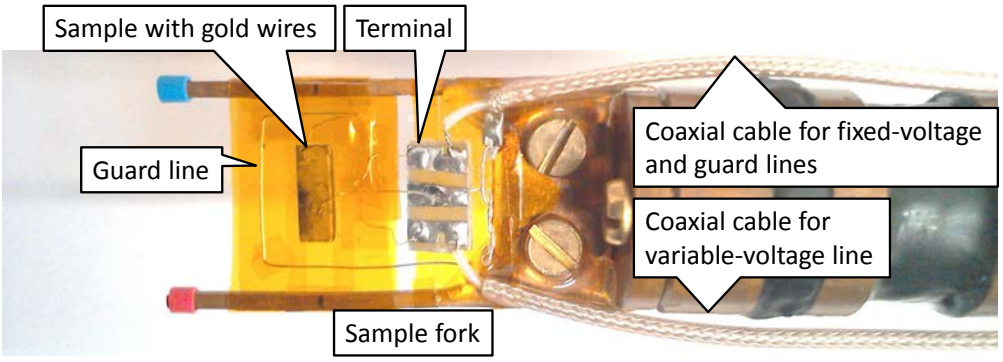

Figure 1: Photograph of the sample rod.

$Cu_3Mo_2O_9$, a quasi-one dimensional slightly canted antiferromagnet, belongs to multiferroic material. Below the phase transition temperature $T_N = 8$ K, this compound displays a slightly canted antiferromagnetic phase accompanied with the ferroelectric polarization [2, 3], i.e., (weak) ferromagnetism and ferroelectricity coexist at 0.1 T. In general, the sublattice magnetization is an order parameter of antiferromagnetic phase transition; Neutron diffraction measurements are usually the tool of choice to study it. Unfortunately, because of the absence of magnetic superlattice formation [4, 5], almost all of the weak magnetic Bragg peaks were superimposed on the strong nuclear ones. Our recent neutron diffraction measurements reported the magnetic structure below T_N [6]. The detailed temperature dependence of the intensity of the magnetic Bragg peaks, however, have not been clarified yet. We focused on the muon spin rotation (μSR) measurement, which is also an efficient method to detect the local internal magnetic field in a crystal [7]. In our previous work at the pulsed muon source at RIKEN-RAL muon facility, we clarified that the μSR spectrum reflects the order parameter of this phase transition and studied the Zn-substitution effects on it. In the parent material, we observed the beating and damping μSR spectrum on a finite background. From the muon oscillating frequencies, we relate the order parameter of the phase below T_N to the amplitudes of internal magnetic fields at the muon stopping site(s). The temperature dependence of the amplitude of internal magnetic field agrees with that of the weak ferromagnetic component in magnetization at 0.1 T. In the 0.5% Zn-doped sample, the increase of magnetization below T_N was not observed at 0.1 T. Even in this case, the μSR spectrum was clearly observed. This fact indicates the effectivity of μSR measurements of this material. In this work, we developed an electric-field application system for the Dolly spectrometer at the Swiss Muon Source to study the cross correlation effects in this material.

2 Experiments

Figure 1 shows the sample setting at the cold end of the sample stick for the Dolly spectrometer. A single crystal of $Cu_3Mo_2O_9$ was prepared using a continuous solid-state reaction technique [8], which was used in our previous μSR measurement at the pulsed muon source at RIKEN-RAL[7]. We prepared a capacitor-shaped single crystal with a thickness of 615 μm, of which wide surfaces perpendicular to the c axis of the crystal were covered by spattered gold. Along

the c axis, the spontaneous electric polarization appears [3]. The sample was set on a sample stage made from Kapton tape between two tines of sample fork, which is conventional way to set the sample at this spectrometer. To connect the sample to the terminal electrically, we used gold wires with a diameter of 25 μm fixed using gold paint. Two coaxial cables connect the terminal to a Keithley Model 6487A Picoammeter/Voltage Source (up to 500 V). Using this pico ammeter, we can monitor the current leakage in real time. Moreover, in case of ferroelectric compound, the pyroelectric current flows into/from the sample when the electric polarization is changed. Using it, we confirmed that the electric junctions work even at low temperatures.

The voltage of the sample surface where the muons are implanted, namely the backward surface, is changed while the voltage of the other surface, namely the forward surface, is fixed to be zero. Here we named the directions, backward and forward, to stay consistent with the directions of muon counters. We set the guard line around the sample to keep the cryostat safe from direct spark from the sample. The guard line is connected to the electrical ground through the shield of the coaxial cable for the fixed-voltage line. The surface of the sample was covered with another Kapton tape. A part of implanted muons might be stopped on this Kapton tape, the gold paint, the thin gold wires, and the spattered thin layer of gold. Hereafter, we call them 'addenda'. This term is popularly used in the field of specific-heat measurements. As will be mentioned later, most of implanted muons are stopped in the sample. Muon spin rotation spectra under electric fields were measured using a standard backward-forward asymmetry technique. We obtained the spectra under voltages (electric fields) of 307 V (0.5 MV/m) and 61 V (0.1 MV/m) together with that at zero electric field. A typical leaked electric current is in the order of 10 pA, corresponding to an electric power in the order of 1 nW. Accordingly, the temperature rise due to the leaked current is negligible. A direct spark was not detected through all measurements. A voltage of 307 V is at almost upper limit of this measurement. Indeed, a current leaking through the sample (due to isolation breakdown) was detected when we applied a voltage of 350 V. The WiMDA software was employed for data analysis [9].

3 Results and Discussion

The left panel of Fig. 2 shows the time-domain backward and forward asymmetry spectra of the $Cu_3Mo_2O_9$ single crystal with the addenda below and above T_N. At 10 K, above T_N, we observed a strong slow oscillation with a period associated with an external transverse magnetic field of 20 G, which indicates that all the muons rotate along the external transverse magnetic field. At 1.5 K, below T_N, we observed a rapid oscillation superimposed on a slow damping oscillation. The period of slow damping oscillation corresponds to the external transverse magnetic field. The damping rate of slow oscillation is equal to that above T_N. Its amplitude becomes about 20% of the initial asymmetry, indicating that 20% of the implanted muons are still stopped at the paramagnetic region. In $Cu_3Mo_2O_9$, the static phase separation effect has not been observed. It is, therefore, natural to consider that 20% of the implanted muons stop at the addenda. At the center of the crystal, where muons are implanted into, there exists a layer of gold paint containing small particles made from Au which stops the muon efficiently because of its heavy ionic mass. (As is well known, the implanted muons are stopped efficiently by heavy ions.) Accordingly, we consider that 20% of the implanted muons probably stop at the gold-paint layer; and, thus, we remove this component in the analysis. The subtracted spectrum was normalized by using the value at zero μs in time. At zero magnetic field, the signal from the muons stopping at the addenda can be reproduced with a simple damping function for the following reasons: (i) The period of the rotation becomes infinity; (ii) There are no reasons why the amplitude decay rate may change.

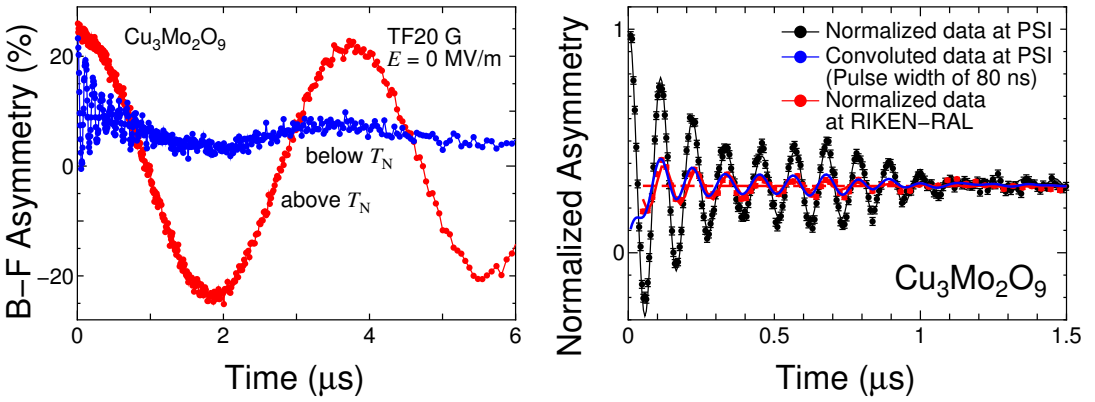

Figure 2: (left, color online) The time-domain backward and forward asymmetry of $Cu_3Mo_2O_9$ single crystal with addenda taken below and above T_N. (right, color online) Comparison between the data taken with continuous and pulsed muon sources. The solid curves connecting the dots in the right panel are the fitted functions (not the smoothed data), of which details are given in text. The red dotted line in the right panel is the underlying background which was necessary for the fitting with two Lorentzians.

After removing the signal from the addenda, we obtained the muon spin rotation spectrum normalized by the signal at zero μs in time, as shown with the black curve in the right panel of Fig. 2. To compare the data with those taken with the pulsed muon source, we need to convolute the present data with the finite pulse width assuming that the muon source had a Gaussian pulse shape. The pulse width is a parameter of this numerical analysis. When we suppose the pulse width as 80 ns, the convoluted spectrum taken with the continuous muon source agrees best with the one taken with the pulsed muon source as shown in the right panel of Fig. 2. This value of the pulse width is consistent with the reported one [10]. Judging from these facts, we consider that the consistency between the present data and the previous ones is good. In our previous paper [7], we reported three components, the almost temperature independent exponentially decaying term, the oscillating term, and the missing term. In this measurement with a continuous muon source, we did not observe the missing term, indicating that the origin of the missing term is the signal broadening due to the convolution effects in the pulsed muon source.

The left and the right panels in Fig. 3 show the time-domain muon spin rotation spectra under electric fields and their fast Fourier transformations, respectively. All of the data are taken under an electric-field cooling condition at zero magnetic field. One can see the beating and damping oscillations in time-domain spectra. The effect of applying an electric field appears as a systematic change in amplitude around 1.6 μs. In the frequency-domain spectra, there exist two peaks with finite linewidth, which correspond to the beating and damping oscillations. Two internal magnetic field strengths are consistent with the previous result [7].

Under electric field, no change in the strengths of internal magnetic fields (peak shifts in a frequency-domain spectrum) were observed. As shown in the right panel of Fig. 3, two peaks in the frequency-domain spectrum were reproduced well by using the Lorentzian function when we suppose the background drawn by a dotted line. The origin of the underlying background in the frequency-domain spectrum is unclear. A fitted spectrum slightly deviates from the fast Fourier transformation; The spectral weight around 700 G seems to show a dip. These prop-

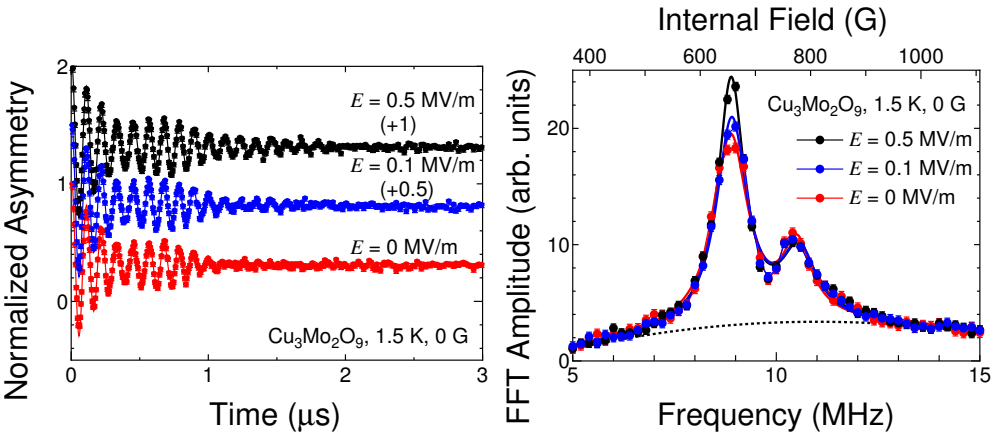

Figure 3: Time- and frequency-domain spectra on the left and the right panels, respectively. The upper scale of the right panel is the strength of the internal magnetic field obtained by multiplication of the muon rotational frequency and the gyromagnetic ratio of muon.

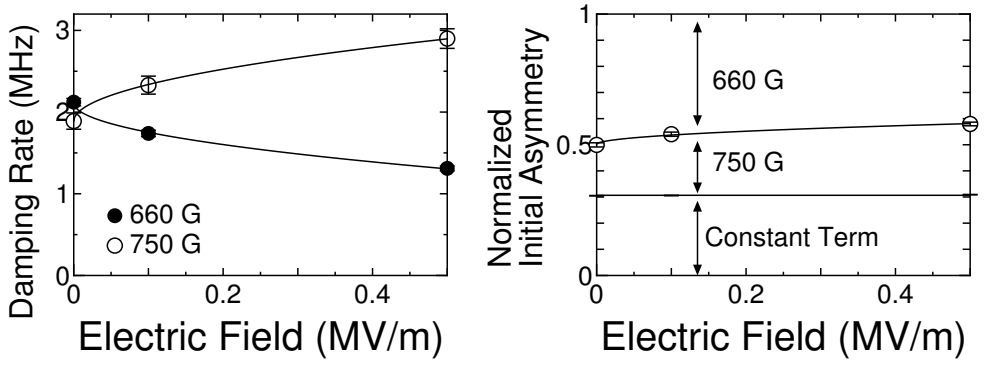

Figure 4: The damping rates and the amplitudes at zero μs in time obtained from the time-domain spectra in the left and the right panels, respectively.

erties indicate that the observed spectrum cannot be explained by two independent damping oscillators at two kinds of muon-stopping sites.

Let us go back to the time-domain spectrum. In spite of the above-mentioned small problems in the frequency-domain spectra, one can see that the overall spectrum has two Lorentzian components. To discuss the beating and damping oscillations, the following function, based on the theory of muon-spin precession around internal fields, is applicable to fit the observed asymmetry spectrum:

$$A(\omega) = \sum_{i=\{1,2\}} A_i \left[\cos^2\theta_i + \sin^2\theta_i \cos\left(\gamma H_i t\right) \exp\left(-\lambda_i t\right)\right] , \tag{1}$$

where A_i, H_i, θ_i, γ, and λ_i are the relative amplitude of the ith mode satisfying that $\sum_i A_i = 1$, the amplitude of the ith internal magnetic field, the angle between the initial spin polarization of muons and the direction of the ith internal magnetic field, the gyromagnetic ratio of muon, and the damping rate of the ith oscillating term, respectively. This fitting function is based on

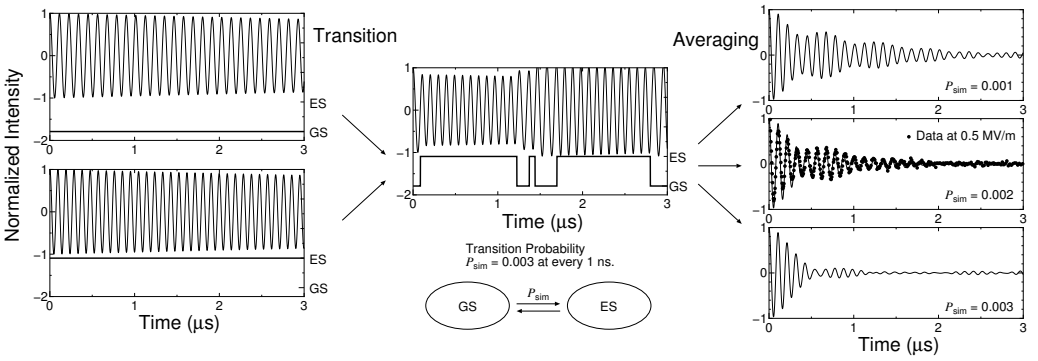

Figure 5: The result of simulation. The top and the bottom panels in the left column show the muon spin spectra rotating along the static internal magnetic fields in the ground and excited states, respectively. As shown in the center panel, the transition effect is introduced with the transition probability $P_{\rm sim}$ of which detailed definition is shown in the test. Averaging approximately one thousand spectra with various transition probabilities are shown in the right column. When we assume $P_{\rm sim}$ as 0.2%, the simulation result reproduces the experimental data qualitatively.

the muon-spin precession around the uniform but slightly fluctuating internal field, which can cause the rapid damping oscillation around the stable averaged value because of fluctuating phase factor. Here we do not introduce a damping factor for the constant term. As shown by solid curves in the left panel of Fig. 3, the observed spectrum is reproduced well by this simple equation. The effects of the background in the frequency-domain spectrum may appear on the rapid damping of the time-domain spectrum around zero μs in time and/or on the high-frequency oscillation with very weak amplitudes. Judging from the value of $\lambda_{\{1,2\}}$ (and the half width of the Lorentzian peak in the frequency-domain spectra), the timescale of the amplitude fluctuation is in the order of 0.1 μs.

From the fitting, we obtained $H_1 = 660$ G and $H_2 = 750$ G, which are consistent with the values in our previous work [7]. The left panel of Fig. 4 shows the damping rate λ_i as functions of the external electric field. One can see that the external electric field stabilizes the 660-G muon-spin precession. The right panel in Fig. 4 shows the relative amplitude of the constant term defined by $\sum_i A_i \cos^2\theta_i$ and $(\sum_i A_i \cos^2\theta_i) + A_2 \sin^2\theta_2$ as functions of the external electric field. The constant term is independent of the external electric field within the experimental accuracy. Judging from the damping rate, the electric-field application stabilizes the muon-spin precession around the 660-G internal magnetic field, while it fluctuates the muon-spin rotation around the 750-G internal magnetic field. Judging from the oscillator strength, the electric-field application seems to stabilize the 750-G oscillation, i.e., these two experimental results seem to contradict each other.

To discuss further, we introduce the following model of a dynamical phase separation, namely the bubble model: (i) The magnetic excited state appears like small bubbles in the sea of the ground state; (ii) The magnetic ground (excited) state gives the 660-G (750-G) internal magnetic field at the muon-stopping site; (iii) The lifetime of the excited state is of the order of 0.1 μs; (iv) The lifetime of the ground state is also in the order of 0.1 μs and it increases with increasing external electric field. We demonstrate that this simple model with only one muon-stopping site can reproduce the experimental data with two muon precession frequencies.

We mapped the muon spin precession on the simple damping harmonic oscillator problem and solve it numerically using the conventional 4th-order Runge-Kutta method. The equation of motion is a simple damping harmonic oscillator. We set the time slice as 1 ns, which reproduces the motion precisely enough. The rotational frequencies are chosen to be associated with the observed internal magnetic fields (660 and 750 G). As shown in the panels in the left column in Fig. 5, the simulation data is sufficiently accurate. We set the damping constant much longer than the time scale of motion. In the following, we studied the effects of magnetic excitation and its decay by introducing a randomly switching rotational frequency. The transition probability $P_{\rm sim}$ for 1 ns is chosen to be 0.3%; e.g., we generate a random number between 0 and 1 at every 1 ns and the state is switched when the value is less than $P_{\rm sim}$. To simulate the muon spin rotation spectrum, we averaged approximately one thousand spectra, which is enough to obtain a steady spectrum. As shown in the panels in the right column, when we assume $P_{\rm sim}$ as 0.2%, the simulation result reproduced the experimental data well. The beating oscillation damps much faster than the decay time of each oscillation because the phase is modulated through the changes of random frequency. The averaged lifetimes of the ground and the excited states are 0.45 μs. This value corresponds to the damping rate of 2.2 MHz, which is consistent with the averaged data in Fig. 4. The oscillation amplitude around 1.5 μs strongly depends on the value of $P_{\rm sim}$. The bubble model can explain the experimental data qualitatively.

We discuss the validity of this model and will point out the issues which should be considered before fitting. In this simulation, we assumed the same $P_{\rm sim}$ for the transitions from the 660 G state to the 750 G one and vice versa. For example, $P_{\rm sim}$s in these two transition processes should be different from each other. This treatment applies for thermodynamic transitions at very high temperature and/or for quantum tunneling. To apply this simulation for a detailed fitting, a more precise treatment is necessary. In the present simulation, we assume that the population of the state with 660 G internal magnetic field is slightly higher than the one with 750 G internal magnetic field. These can be treated as a variable for the fitting. The results in the detailed fitting based on the bubble model will be published elsewhere.

This model is related to the magnetic excitations of $Cu_3Mo_2O_9$, which has been confirmed by the inelastic neutron scattering [4, 5]. We focus on the magnetic excitation at the magnetic zone center. We reported the gapless magnetic excitations with a velocity of approximately 400 m/s, the continuous magnetic excitations with a small spin-gap energy of 1.2 meV, and the discrete gapped mode at 5.8 meV. Hereafter, we discuss the former two magnetic excitations because the energy of the discrete gapped mode is too large to be thermally excited at 1.5 K.

In our previous work [5], the gapless magnetic excitations have been assigned as the des Cloizeaux and Pearson excitation [11]. The magnetic-excitation continuum has been explained by using the interchain mean-field theory [12]. These are the typical features of magnetic excitations in the quasi-one dimensional antiferromagnetic systems. To apply these theories, we had assumed the magnetic structure which was denied by the recent result of the neutron diffraction measurement [6]. Currently, we cannot answer the origin of the magnetic excitations in $Cu_3Mo_2O_9$. In spite of these difficulties, we can consider the following model based on the experimental results in ref. [5].

The existence of the gapless magnetic excitation explains the squeezing of the internal magnetic field. In the observation time (approximately 1 μs), the magnetic excitation propagates 0.4 mm, which is of the order of 1/10 times of the diameter of the beam spot (approximately 5 mm). This can be an origin of the damping of the muon-spin precession around the internal magnetic field of 660 G. At the bottom of the magnetic-excitation continuum, the density of states is large. Thus, we can consider the magnetic excitation at the bottom of the magnetic-excitation continuum as if it has a discrete energy level. Because of the parabolic magnetic dispersion

relation, the magnetic excitation at the bottom of the magnetic excitation continuum is well localized at least in the timescale of muon measurement. This localized excitation creates the 750 G internal magnetic field. These features are consistent with our bubble model. It can be an origin of the internal magnetic field distribution. Under the electric field, according to our experimental result, the number of bubbles increases and the lifetime of bubbles decreases. These can be explained by the reduction of the spin-gap energy, which leads to an increase of the transition probability of thermal activation and an increase of the decay rate from the excited state to the ground state.

Information on the muon-stopping site(s) is also important to discuss the muon decay process. In this work, we implicitly assumed that the muon stopping site is only one kind in this crystal. To prove the validity of this assumption, we need to simulate the muon-stopping site(s) in the crystal. This is beyond this paper. To confirm this model, the temperature and magnetic-field dependences of μSR spectra under electric fields are strongly desired. As we wrote above, we consider that the switching of the internal magnetic field can be the origin of the beating and damping oscillation below T_N. If so, the electric field dependences of the damping factors λ_i should be independent of the initial muon-spin polarization. The spin rotator installed at the Dolly spectrometer enables us to perform this experiment easily; Unfortunately, we have not yet performed this experiment. More detailed studies, including this measurement, are strongly desired.

4 Conclusion

To study cross correlation effects in multiferroic $Cu_3Mo_2O_9$, we developed electric-field application system for the Dolly spectrometer. We observed that the muon spin rotation spectrum systematically changes under electric fields up to 0.5 MV/m. The muon spin rotation time spectrum shows beating and damping oscillations, suggesting that two kinds of internal fields exist. However, the frequency-domain analysis shows that the observed spectrum cannot be explained based on two independent oscillators. To explain the results of the asymmetry spectrum, we introduced a model with one muon-stopping site. This model is based on the experimental results of the inelastic neutron-scattering experiments in $Cu_3Mo_2O_9$.

References

[1] T. Kimura, T. Goto, H. Shintani, K. Ishizaka, T. Arima, and T. Tokura: Nature **426** (2003) 55.

[2] T. Hamasaki, N. Ide, H. Kuroe, T. Sekine, M. Hase, I. Tsukada, and T. Sakakibara: Phys. Rev. B **77** (2008) 134419.

[3] H. Kuroe, T. Hosaka, S. Hachiuma, T. Sekine, M. Hase, K. Oka, T. Ito, H. Eisaki, M. Fujisawa, S. Okubo, and H. Ohta: J. Phys. Soc. Jpn. **80** (2011) 083705.

[4] H. Kuroe, T. Hamasaki, T. Sekine, M. Hase, K. Oka, T. Ito, H. Eisaki, and M. Matsuda: J. Phys.: Conf. Ser. **200** (2010) 022028.

[5] H. Kuroe, T. Hamasaki, T. Sekine, M Hase, K. Oka, T. Ito, H. Eisaki, K. Kaneko, N. Metoki, M. Matsuda, and K. Kakurai: Phys. Rev. B **83** (2011) 184423.

[6] M. Hase, H. Kuroe, V. U. Pomjakushin, L. Keller, R. Tamura, N. Terada, Y. Matsushita, A. Dönni, and T. Sekine, Phys. Rev. B **92** (2015) 054425.

[7] H. Kuroe, K. Aoki, T. Sato, R. Kino, H. Kuwahara, T. Sekine, M. Hase, I. Kawasaki, T. Kawamata, T. Suzuki, I. Watanabe, K. Oka, T. Ito, and H. Eisaki: JPS Conf. Proc. **2** (2014) 010206.

[8] K. Oka, T. Ito, H. Eisaki, M. Hase, T. Hamasaki, H. Kuroe, and T. Sekine: J. Cryst. Growth **334** (2011) 108.

[9] F. L. Pratt: Physica B **289-290** (2000) 710.

[10] T. Matsuzaki, K. Ishida, K. Nagamine, I. Watanabe, G. H. Eaton, and W. G. Willams: Nucl. Instr. and Meth. A **465** (2001) 365.

[11] J. des Cloizeaux and J. J. Pearson: Phys. Rev. **128** (1962) 2131.

[12] H. J. Schulz: Phys. Rev. Lett. **77** (1996) 2790.